Low-Complexity Blind Phase Search for Filter Bank Multicarrier Offset-QAM Optical Fiber Systems

Trung-Hien Nguyen[1], Simon-Pierre Gorza[1], Jérome Louveaux[2] and François Horlin[1]
[1] *OPERA department, Université libre de Bruxelles, Belgium*
[2] *ICTEAM Institute, Université catholique de Louvain, Belgium*
E-mail: Trung-Hien.Nguyen@ulb.ac.be

Abstract: A low-complexity blind phase search (BPS) for the carrier phase estimation in optical FBMC-OQAM systems is proposed. Compared to the BPS algorithm, the proposed method is of lower complexity while still delivering a similar performance.
OCIS codes: (060.1660) Coherent communications; (060.4080) Modulation; (060.2360) Fiber optics links and subsystems.

1. Introduction

Filter bank multicarrier offset quadrature modulation format (FBMC-OQAM) is an interesting alternative to orthogonal frequency-division multiplexing (OFDM) and has recently received much attention in optical fiber communication systems [1-3] thanks to its optimized spectral efficiency (SE) and its robustness to the channel variation in optical fibers. On each subcarrier of FBMC-OQAM systems, a half-symbol time delay between the in-phase and quadrature components of the signal is introduced, in order to achieve the orthogonality between adjacent subcarriers [4]. However, in the presence of the laser phase noise, inter-carrier interference appears between the OQAM subcarriers in addition to the corresponding rotation [5]. As a consequence, the frequently-used carrier phase estimation (CPE) methods for QAM constellations are no longer suitable, unless the laser linewidth is of several kHz [4]. Several CPE solutions for OQAM signals have been proposed so far. The pilot used in [4] can be exploited to the CPE, however, suffering from the reduced SE. An innovative phase tracking combined with the equalizer has been reported in [1], at the cost of extra feedback loop delay. Recently, the modified blind phase search (M-BPS) has recently been proposed in [5], taking the advantage of the feedforward operation [6]. However, the computation effort (CE) is increased associated with the increase of the OQAM modulation level.

In this paper, a modified BPS of lower complexity (LC-BPS) is proposed for FBMC-OQAM systems, in which the distance calculations in the complex plane in M-BPS method is replaced by simple multiplication-free operations in the real plane. Moreover, a modified phase searching strategy is also applied, leading to further reduction of the CE. The proposed methods are numerically validated in a 5-subcarriers FBMC-16OQAM system. Similar to M-BPS method, the tolerated normalized linewidth (the product of laser linewidth and symbol duration) of the LC-BPS method is 10^{-4} for a 1 dB SNR penalty of BER=10^{-3} with about twice the reduction of CE.

2. Low-complexity feedforward carrier phase estimation

The idea behind the modified BPS for OQAM signals is to pre-rotate the received samples with a number of phase tests before removing the half-symbol delay between the in-phase and quadrature components of the received signals [5]. Fig. 1 presents a block diagram of the modified BPS algorithm. As the conventional BPS, the input samples (before applying the standard OQAM equalization) at twice symbol-rate, *r*, are firstly rotated by test phase value $\phi_b = (b/B)\cdot\pi - \pi/2$, where b = 1, 2, …, B and B is the total number of the phase tests.

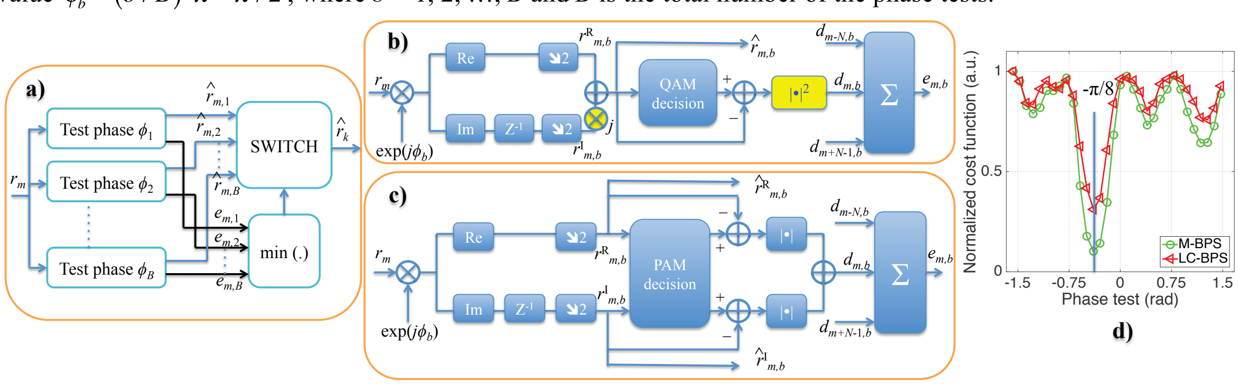

Fig. 1. Block diagram of modified blind phase search (M-BPS) for OQAM signals. Test phase blocks for b) M-BPS and c) low-complexity LC-BPS without multiplier operator in the cost function calculation. d) Cost functions of M-BPS and LC-BPS for a phase noise value of $\pi/8$.

The rotated m-th sample of the k-th subcarrier can be represented by $r_{k,m,b} = r_{k,m} \cdot \exp\left(j \cdot \phi_b\right)$. To simplify the notation, the subcarrier index is omitted later. The rotated samples version (Fig. 1(a)) corresponding to each phase test is then sent to a switch, in order to select the best phase rotation to alleviate the phase noise impact. The rotated phase is chosen if it minimizes the cost function, $d_{m,b}$. The impact of the additive noise is reduced by averaging the cost function over $2N$ consecutive samples with the same phase test, $e_{m,b} = \sum_{n=-N}^{N-1} d_{m+n,b}$. Fig. 1(b) and (c) show the operations inside each test phase block for M-BPS and LC-BPS, respectively. The expected phase rotation with respect to the phase noise suppression can be expressed by

$$\begin{aligned} \hat{\phi}_{b,\text{M-BPS}} &= \arg\min_{\phi_b} e_{m,b,\text{M-BPS}} = \arg\min_{\phi_b} \sum_{n=-N}^{N-1} \left(\left| r_{m+n,b} - DD\left(r_{m+n,b}\right) \right|^2 \right), && \text{for M-BPS} \\ \hat{\phi}_{b,\text{LC-BPS}} &= \arg\min_{\phi_b} e_{m,b,\text{LC-BPS}} = \arg\min_{\phi_b} \sum_{n=-N}^{N-1} \sum_{l=1}^{2} \left(\left| r^l_{m+n,b} - DD\left(r^l_{m+n,b}\right) \right| \right), && \text{for LC-BPS} \end{aligned} \tag{1}$$

in which DD is the direct decision operator. $r^1_{m,b}= r^R_{m,b}$ and $r^2_{m,b}= r^I_{m,b}$ are the real and imaginary parts of the samples, respectively. Note that, the distance calculations in the complex plane in the M-BPS require 2 real-multiplications and 3 real-additions. It is clearly seen that the 2 real-multiplications are removed in the proposed LC-BPS, resulting in the reduced CE compared to the traditional M-BPS. Fig. 1(d) shows the examples of cost functions for M-BPS and LC-BPS method at the phase noise value of $\pi/8$. It can be observed that the 2 cost functions exhibit the same minimum value at about $-\pi/8$. A new searching-strategy, referred to as SLC-BPS, can be used to reduce further the CE. More particularly, the coarse phase search (CPS) is firstly carried out with half of the required phase test numbers, the fine phase search (FPS) will compare the minimum cost function value (with respect to $\hat{\phi}_b$, found by CPS) to the two adjacent cost function values at the two adjacent phases (i.e. $\hat{\phi}_b \pm \pi/28$ explained later). As a result, the required total number of phase tests is (B/2+2), or equivalently the total number of operators is reduced to B/(B/2+2) times, approximated 2 times when B is large. Further CE reduction is feasible by cascading several CPS stages. Because the cost function exhibits several local minima (Fig. 1(d)), the number of cascaded CPS stages should be optimized but the detail investigation is out of the scope of this paper. Table. I summarizes the required operations for different CPE methods in a block length, 2N, with B phase test values. For a fair comparison, only the operations required for the cost function calculation are taken into account.

Table I. Computational complexity for M-BPS, MF-BPS and SLC-BPS

	Real multiplication	Real addition	Decision
M-BPS	4NB	6NB	4NB
LC-BPS	–	6NB	4NB
SLC-BPS	–	3NB+4N	2NB+4N

N – half of the summation block length; B – number of phase test values.

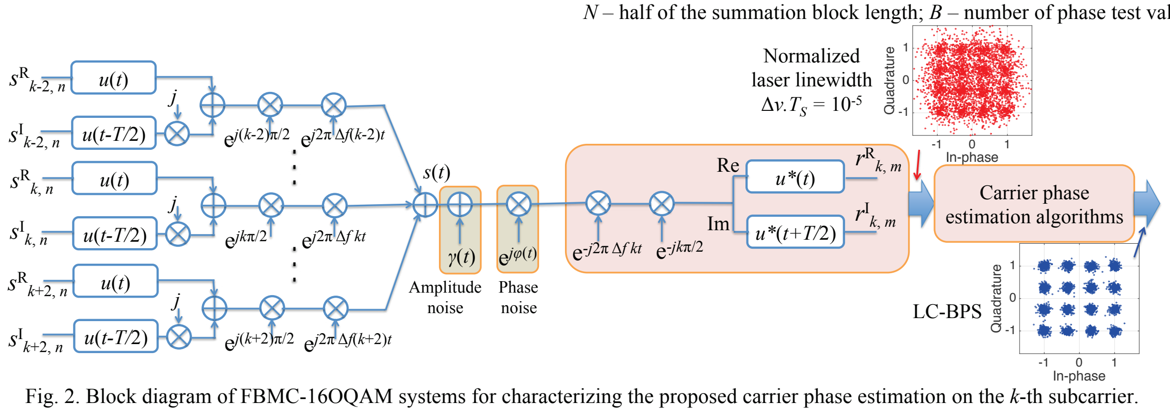

Fig. 2. Block diagram of FBMC-16OQAM systems for characterizing the proposed carrier phase estimation on the k-th subcarrier.

3. Results and discussion

The performance of the proposed CPE methods is numerically studied with 5-subcarriers FBMC-16OQAM optical coherent systems. To focus on the laser phase noise impact, only one polarization is studied and other impairments (i.e. chromatic dispersion, frequency offset) are assumed to be completely compensated. Fig. 2 presents the block diagram used for the simulations. The 16OQAM signals on each subcarrier are generated by differential encoding, mapping the random binary sequences on the QAM constellation and staggering a half of symbol time between the in-phase and quadrature components. These signals are pulse-shaped with square-root raised cosine (SRRC, roll-off factor of 1) filters, $u(t)$, before imprinting onto the subcarriers. Note that, a $\pi/2$ phase difference is introduced between adjacent subcarriers to ensure the orthogonality. All the subcarriers are then summed up together to form a total 130 000 FBMC-16OQAM symbols. These symbols are then corrupted by additive Gaussian white noise (AWGN), $\gamma(t)$, and loaded with the laser phase noise, $\varphi(t)$. The phase noise is modeled as a discrete random time walk $\varphi_m = \varphi_{m-1} + \Theta_m$, where Θ_m is a zero-mean Gaussian random variable with variance of $2\pi \cdot \Delta\nu \cdot T_S$. $\Delta\nu$ and T_S denote the laser linewidth and symbol duration, respectively. At the receiver (see Fig. 2), the subcarrier frequency is firstly removed and then compensated for the $\pi/2$ phase difference between adjacent subcarriers. After that, the signals are passed to the matched SRRC filter. Finally, the output signal samples are used to evaluate the effectiveness of proposed CPE algorithms.

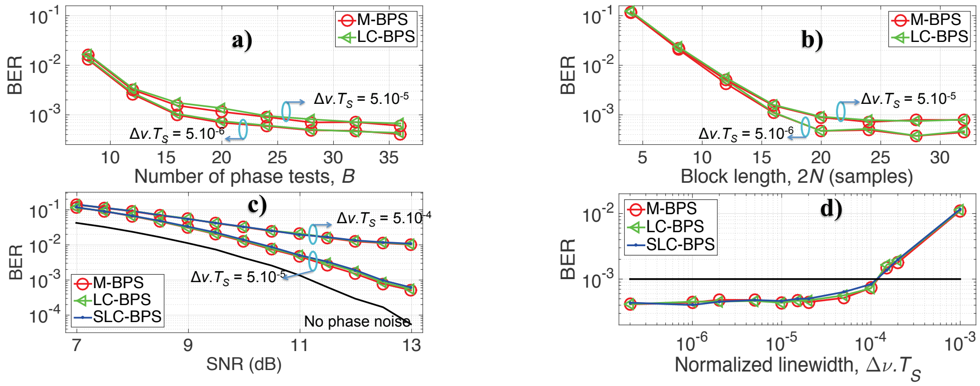

Fig. 3. a) Calculated BER versus number of phase tests and b) calculated BER versus block length for two normalized linewidths of $5\cdot10^{-5}$ and $5\cdot10^{-6}$. c) BER as a function of SNR for two normalized linewidths of $5\cdot10^{-4}$ and $5\cdot10^{-5}$. d) BER versus normalized linewidth.

Fig. 3(a) shows the calculated bit-error ratio (BER) as a function of the number of phase tests, B, at normalized linewidths, $\Delta\nu \cdot T_S$, of $5\cdot10^{-5}$ and $5\cdot10^{-6}$. It can be observed that the BER firstly deteriorates and then remains constant with the increase of B. The optimum number of phase tests for 16OQAM signals are 28 and are not affected by changing the normalized linewidth. For this reason, we use two adjacent phase test values of the minimum deduced phase $\hat{\phi}_b$ (in SLC-BPS) being $\hat{\phi}_b \pm \pi/28$. The impact of the summation block length, $2L$, is further studied in Fig. 3(b) for two normalized linewidths of $5\cdot10^{-5}$ and $5\cdot10^{-6}$. It can be seen that the minimum block length (defined as the shortest block length enabling to reach the target BER) for 16OQAM signals are 20 regardless of the laser linewidth.

In the next step, the evolution of BER at different SNRs is shown in Fig. 3(c) for different methods at the normalized linewidths of $5\cdot10^{-4}$ and $5\cdot10^{-5}$. The calculated BER decreases when increasing the SNR, all three methods have the same performance. However, at 10^{-2} BER, the algorithm performance for the high-normalized linewidth ($5\cdot10^{-4}$) case exhibits a 1.8 dB SNR penalty compared to that of the low-normalized linewidth ($5\cdot10^{-5}$) case. Note that, compared to the absence of the phase noise, there always exists a 1.2 dB SNR penalty after the CPE inherent to the traditional BPS algorithm [6]. The tolerated normalized linewidth of the algorithms at 12.2 dB SNR (which is 1 dB above the SNR reaching the target BER=10^{-3}) is further investigated in Fig. 3(d). The BER remains constant as long as the normalized linewidth is smaller than $5\cdot10^{-5}$ and starts to increase for higher linewidths. Once again, the evolutions of all three algorithms are superimposed, confirming the effectiveness of the proposed low-complexity CPEs. It is clearly seen that the CPE algorithms for 16OQAM signals can tolerate the normalized linewidth of 10^{-4}, while our proposed methods reduce much computational effort, compared to the traditional M-BPS method.

4. Conclusion

A low-complexity modified blind phase search (BPS) algorithm for OQAM signals has been proposed and numerically validated with 5-subcarriers FBMC-16OQAM systems. The proposed method provides a tolerated normalized linewidth of 10^{-4} for a 1 dB SNR penalty at BER=10^{-3}, as the BPS with reduced computational effort.

5. Acknowledgment: This work is supported by the Belgian Fonds National de la Recherche Scientifique – FNRS (PDR T.1039.15).

6. References

[1] J. Fickers, et al., "Multicarrier offset-QAM for long-haul coherent optical communications," J. Lightw. Technol. **32,** 4069-4076 (2014).
[2] S. Randel, et al., "Generation of 224-Gb/s multicarrier offset-QAM using a real time transmitter," in Proc. OFC (2014), p. OM2H.2.
[3] F. Horlin, et al., "Dual-polarization OFDM-OQAM for communications over optical fibers …," Opt. Express **21**, 6409-6421 (2013).
[4] J. Zhao, "DFT-based offset-QAM OFDM for optical communications," Opt. Express **22**, 1114-1126 (2014).
[5] H. Tang, et al., "Feed-forward carrier phase recovery for offset-QAM Nyquist WDM transmission," Opt. Express **23**, 6215-6227 (2015).
[6] T. Pfau, et al., "Hardware-efficient coherent digital receiver concept with feedforward carrier …," J. Lightw. Technol. **27**, 989-999 (2009).